Structural Engineering and Mechanics, Vol. 3, No. 5 (1995) 445-462
DOI: http://dx.doi.org/10.12989/sem.1995.3.5.445

Yield mechanisms of stepped cantilevers subjected to a dynamically applied constant tip force

B. Wang†

School of Mechanical and Production Engineering, Nanyang Technological University, Singapore 2263

Abstract. Previous studies of a stepped cantilever with two straight segments under a suddenly applied constant force (a step load) applied at its tip have shown that the validity of deformation mechanisms is governed by certain geometrical restrictions. Single and double-hinge mechanisms have been proposed and it is shown in this paper that for a stepped cantilever with a stronger tip segment, i.e. $M_{0.1}>M_{0.2}$, where $M_{0.1}$ and $M_{0.2}$ are the dynamic fully plastic bending moments of the tip and root segments, respectively, the family of possible yield mechanisms is expanded by introducing new double and triple-hinge mechanisms. With the aid of these mechanisms, it is shown that all initial deformations can be derived for a stepped cantilever regardless of its geometry and the magnitude of the dynamic force applied.

Key words: dynamic plasticity; impact; plastic hinges; stepped cantilever; pipe whip.

1. Introduction

In a typical high pressure piping system, such as those in a nuclear power station, a sudden rupture may cause an unbalanced load due to the escaping fluid which results in a sudden motion of the pipe. This phenomenon is called pipe whip. Modeling the deformation of a pipe run under pipe whip is a complex problem. The simplest approach is to formulate a small deflection analysis in which the pipe is treated as a rigid-perfectly plastic cantilever beam under an end load. The effect of geometry change and material elasticity are neglected in the governing equations and axial forces are normally ignored. This leads to substantial simplification of the analysis and gives useful guidance for design purpose. Different beam configurations, such as straight, circular and bent cantilevers have been analyzed under this approach in the literature in order to provide insight into pipe whip responses, see Lee and Symonds (1952), Martin (1964), Yu, *et al.* (1985), Wang, *et al.* (1993), Wang (1994) and Reid, *et al.* (1995a, b).

The problem considered in this paper is a stepped cantilever with two straight segments, designated as AC and CB, under a step load applied transversely at its tip A. Based on the small deflection and rigid-perfectly plastic material assumptions, this problem was first analyzed by Hua, *et al.* (1988) for those with $M_{0.1}<M_{0.2}$, where $M_{0.1}$ and $M_{0.2}$ are the dynamic fully plastic bending moments of the tip and root segments AC and CB, respectively. But for a stepped cantilever with $M_{0.1}>M_{0.2}$, no complete family of solutions has been obtained. It is intended in this paper to discuss deformation modes more complex than the double-hinge ones given by Hua, *et al.* (1988). All possible yield mechanisms are discussed in this study under various geometrical and loading conditions. As such, it provides a complete family of solutions for a stepped cantilever with $M_{0.1}>M_{0.2}$.

† Lecturer

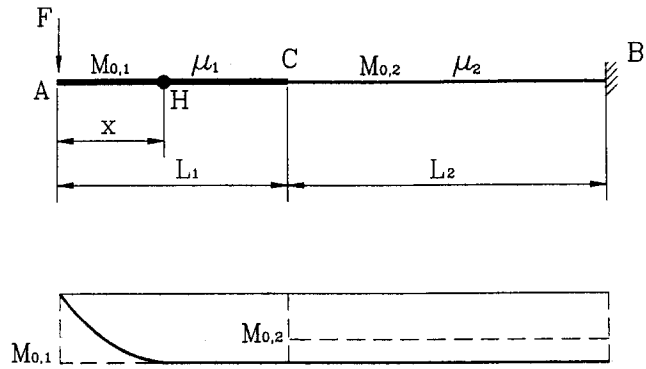

Fig. 1 Bending moment diagram for a single hinge mode with the hinge assumed in AC.

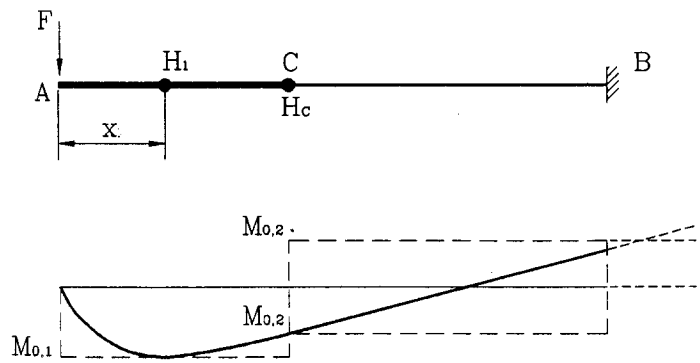

Fig. 2 Bending moment diagram for a double-hinge mode with the hinges in AC and at C, respectively.

The invalidity of a single hinge mechanism for a stepped cantilever under a step tip load was first discussed by Hua, *et al.* (1988), as shown in Fig. 1. If the dynamic fully plastic bending moments in segment AC, $M_{0,1}$ is larger than that in CB, $M_{0,2}$, when the magnitude of the suddenly applied tip load F is high enough, a hinge would appear in AC and the yield criterion would be violated in segment CB. To solve this problem, Hua, *et al.* introduced a double-hinge mechanism, indicating that two plastic bending hinges appear simultaneously in segment AC and at connection C, as shown in Fig. 2. However the validity of this mode is governed by the length of CB. As the shear force at C, Q_C is not zero, the yield criterion may be violated at B when CB is beyond a certain length. The validity of this double-hinge mechanism requires,

$$Q_C L_2 - M_{2,0} \leq M_{2,0},$$

or

$$L_2 \leq \frac{4M_{0,2}(L_1 - x)}{3(M_{0,1} - M_{0,2})} \tag{1}$$

where L_1 and L_2 are the lengths of AC and CB, respectively, and x is the hinge position in AC determined by Eq. (13) of Hua, *et al.* (1988).

To remove the above constraint, and as will be discussed in the following, to investigate the

aspects which Hua, *et al.* (1988) had not discussed, new double- and triple-hinge modes are proposed in this paper. It will also be shown that these new mechanisms are all complete solutions, viz. satisfy all the kinetic conditions and the yield criterion. Furthermore, it shows that with the new modes, a complete family of yield mechanisms is constructed for a stepped cantilever with $M_{0,1}>M_{0,2}$ under a step tip load. No further yield mechanism is needed.

As stated above, the current study is based on the assumption that the cantilever is made from rigid-perfectly plastic materials and each straight beam segment has a uniform section and density. The deflection is small so only initial phase of the response is considered. This small deflection analysis is particularly useful in revealing the initial positions of the plastic hinges where the failure begins. And the idealized material model greatly simplifies the analysis while maintains the main issue of the problem. Also the analysis assumes that the dynamic load, F is a step load, i.e. a suddenly applied constant force at the beam tip, and the shear force Q is neglected in the yield criterion.

For the development of the paper, we follow the increasing magnitude of the step load F. We first introduce a single hinge mode, then examine the situation where the yield criterion is violated. This violation leads to the derivation of three different double-hinge mechanisms. Further increase in the magnitude of the step load results in the invalidity of these double-hinge modes and raises the necessity of three-hinge mechanisms. The analysis is always carried out in the following four steps:

(1) It is assumed that one, two or even three hinges may form somewhere simultaneously in the beam segments for a single, double or triple-hinge mechanism, respectively.
(2) Based on the free-body diagram obtained by cutting the beam segments at the supposed hinge locations and using d'Alembert's principle, one translational and one rotational equations are obtained for each segment;
(3) After eliminating the terms of angular accelerations, an expression relating the step load and hinge positions is obtained;
(4) The following conditions are checked:
   a. the yield criterion in each beam segment is not violated;
   b. the angular acceleration is in the assumed direction;
   c. the hinge position obtained is inside the segment concerned.

Some of these conditions will produce a range of load in which a particular mode is valid, or impose a restriction on the geometry of the beam.

It is necessary to emphasis again that the present paper is restricted to the cantilevers with $M_{0,1}>M_{0,2}$. For those with $M_{0,1}=M_{0,2}$ and $M_{0,1}<M_{0,2}$, refer to Johnson (1972) and Hua, *et al.* (1988), respectively.

2. Theoretical modeling

2.1. Single hinge mechanism

For completeness and in order to provide an insight into the problem, a single hinge mechanism is first examined. A simple static analysis shows that when

$$F<F_0=\frac{M_{0,2}}{L_1+L_2}, \tag{2}$$

there would be no yield in the beam. If $F\geq F_0$, a hinge may appear at beam root B or in

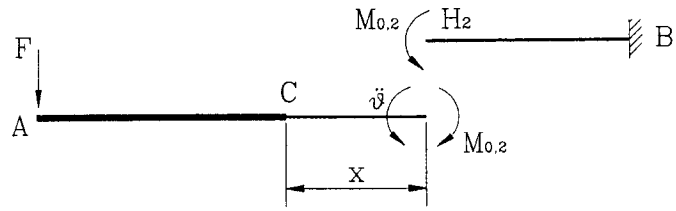

Fig. 3 Single hinge mode H_2.

segment CB. Assuming that a hinge is formed in CB at x measured from C, as shown in Fig. 3, the equations of translational and rotational motions are given as

$$F=\frac{\mu_1}{2}\left[(L_1+x)^2-x^2\right]\ddot{\vartheta}+\frac{\mu_2}{2}x^2\ddot{\vartheta}, \tag{3}$$

$$F(L_1+x)-M_{0,2}=\frac{\mu_1}{3}\left[(L_1+x)^3-x^3\right]\ddot{\vartheta}+\frac{\mu_2}{3}x^3\ddot{\vartheta}, \tag{4}$$

where μ_1 and μ_2 are the densities of unit length of segment AC and CB, respectively, $\ddot{\vartheta}$ is the angular acceleration at the hinge.

Combining the above equations produces,

$$F=\frac{3M_{0,2}[\mu_1(L_1+2x)L_1+\mu_2x^2]}{\mu_1(L_1+3x)L_1^2+\mu_2(3L_1+x)x^2} \tag{5}$$

This is the relationship between the hinge position and the magnitude of the force applied at the beam tip. substituting $x=L_2$ and 0 into Eq. (5) gives the force magnitudes when a hinge is formed at B and C, respectively,

$$F_1=F(L_2)=\frac{3M_{0,2}[\mu_1(L_1+2L_2)L_1+\mu_2L_2^2]}{\mu_1(L_1+3L_2)L_1^2+\mu_2(3L_1+L_2)L_2^2} \tag{6}$$

and

$$F_2=F(0)=\frac{3M_{0,2}}{L_1} \tag{7}$$

These correspond to the highest and lowest magnitude of the dynamic force for a single hinge to appear in CB. It is clear now that with $F_0\leq F\leq F_1$, a plastic hinge will form at B and with $F_1<F<F_2$, a hinge will form in CB with the position determined by Eq. (5), and with $F=F_2$, the hinge will appear at C. Because $M_{0,1}>M_{0,2}$, the hinge at C will be formed at the end of CB connected with AC with the bending moment being $M_{0,2}$. It is not difficult to prove that as long as $F\leq F_2$, the validity of this single hinge mode is always maintained since there is no violation of the yield criterion anywhere in the beam.

With $F\geq F_2$, assuming that a hinge is still formed at C, the shear force at C, Q_C, will not be zero. As shown in Fig. 4, the governing equations of the beam are,

$$F-Q_C=\frac{\mu_1}{2}L_1^2\ddot{\vartheta}, \tag{8}$$

$$FL_1-M_{0,2}=\frac{\mu_1}{3}L_1^3\ddot{\vartheta}. \tag{9}$$

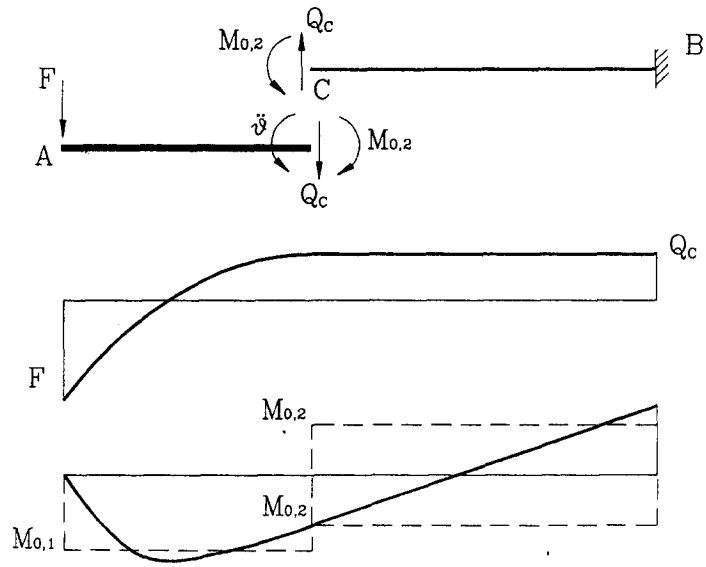

Fig. 4 Shear force and bending moment diagram for a single hinge mode at C indicating possible yield criterion violations in AC and CB when $F>F_2$.

Eliminating $\ddot{\vartheta}$ from Eqs. (8) and (9) gives

$$F=\frac{3M_{0,2}}{L_1}-2Q_C.$$

Combining the above expression with Eq. (7) gives

$$Q_C=\frac{1}{2}(F_2-F) \tag{10}$$

Eq. (10) shows that the shear force at C is zero only with $F=F_2$ and when $F>F_2$, Q_C becomes non-zero and turns to the opposite direction of F. When this happens there appears three possible violations of the yield criterion. First, the maximum value of the bending moment will happen in AC rather than at C, thus it may exceed $M_{0,1}$ if F is large enough, as indicated by Fig. 4; and second, since Q_C is not zero, the yield condition at B or in CB may be violated if CB is long enough, or thirdly, violations in both AC and CB may happen simultaneously. Therefore, it is necessary to check the yield condition in both AC and CB respectively for the validity of this single hinge mode.

First assuming that the yield criterion in CB is not violated and ξ is an arbitrary point in AC measured from A. For segment Aξ, the governing equations of motion for a single hinge mode at C produce

$$F-Q_\xi=\mu_1\xi\left(L_1-\frac{\xi}{2}\right)\ddot{\vartheta} \tag{11}$$

and

$$F\xi-M_\xi=\frac{\mu_1}{2}\xi^2\left(L_1-\frac{\xi}{3}\right)\ddot{\vartheta}. \tag{12}$$

If M_ξ reaches the maximum at ξ, $Q_\xi=0$. From Eqs. (9), (11) and (12), we have

$$M_\xi = \frac{\xi^2\left(\frac{L_1}{2} - \frac{\xi}{3}\right)M_{0.2}}{L_1\left[\xi\left(L_1 - \frac{\xi}{2}\right) - \frac{L_1^2}{3}\right]} \tag{13}$$

and

$$F = \frac{(2L_1 - \xi)M_\xi}{\left(L_1 - \frac{2}{3}\xi\right)\xi} \tag{14}$$

Eliminating ξ from Eqs. (13) and (14) gives the relationship $F = F(M_\xi)$. And let $M_\xi < M_{0.1}$, we have the condition for no violation of the yield criterion in AC

$$F < F_3 = F(M_{0.1}) \tag{15}$$

No closed-form expression of F_3 can be achieved and from Eqs. (13) to (15), we may see that F_3 is a function only decided by beam parameters L_1, $M_{0.1}$ and $M_{0.2}$. It is understood that when $F_2 \leq F < F_3$, a valid single hinge mode at C will appear; and when $F \geq F_3$, the yield criterion at ξ in AC will be violated and a new mode should be introduced. Typically, this can be done by assuming an additional hinge appearing at the point where the maximum bending moment occurs. It should be noted that with the new hinge introduced, all governing equations should be re-derived and the yield criterion in each beam segment re-examined. This will be shown in the following sections.

Now we check the yield criterion at B for the single hinge mode at C. Assume that there is no violation of the yield criterion in AC, for segment CB, we have

$$Q_C L_2 - M_{0.2} = M_B. \tag{16}$$

If $M_B < M_{0.2}$, the above equation gives

$$F < F_4 = F_2 + 2Q_C = F_2 + \frac{4M_{0.2}}{L_2} = \left(\frac{3}{L_1} + \frac{4}{L_2}\right)M_{0.2}. \tag{17}$$

This is the condition for no violation of the yield criterion at B. With Eqs. (15) and (17) both satisfied, there is no violation anywhere in the stepped beam and the single hinge mechanism at C remains valid.

Comparisons between the values of F_3 and F_4 are difficult. When $L_2 \to \infty$, we have $F_4 \to F_2 (< F_3)$; and when $L_2 \to 0$, it gives $F_4 \to \infty (> F_3)$. Thus there exists a limiting length of CB. When L_2 is longer than the limit, with $F > F_4$, B may fail simultaneously with C, indicating that a double-hinge mode C-B will appear, also there is a possibility that a failure occurs in CB rather than at B so a C-H_2 mode appears; or when L_2 is less than the limit, AC may fail simultaneously with C if $F > F_3$ and this leads to a double-hinge mode H_1−C. In the following section the length limit of CB and these double-hinge modes are discussed.

2.2. Double-hinge mechanisms

The single hinge mechanism has shown some restrictions on its validity and this leads to the need for double-hinge mechanisms. The double-hinge mechanisms can be analyzed similarly and their validity needs to be examined as well. There are three possible double-hinge modes, i.e. H_1−C, C−H_2 and C−B modes, corresponding to the violation of the yield criterion in segment AC, CB and at B, respectively when the single hinge is at C. It will be shown that

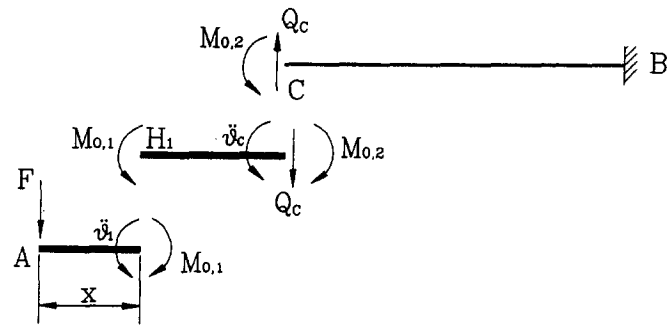

Fig. 5 Double-hinge mode H_1-C.

these double-hinge mechanisms are all valid but subjected to some restrictions as well and further hinges are needed to be introduced into the system.

2.2.1. H_1-C mode

Assuming that under the dynamic tip load, there appears a hinge, H_1 at x measured from A in AC and at C simultaneously in the stepped beam, as shown in Fig. 5. The relative angular velocities at the hinges are $\ddot{\vartheta}_1$ and $\ddot{\vartheta}_C$, respectively. Employing d'Alembert's principle, the governing equations for segment H_1C are

$$Q_C=\frac{\mu_1}{2}(L_1-x)^2\ddot{\vartheta}_C, \tag{18}$$

$$M_{0,1}-M_{0,2}=\frac{\mu_1}{3}(L_1-x)^3\ddot{\vartheta}_C. \tag{19}$$

For segment AH_1, we have

$$F=\mu_1 x\left(\left(L_1-\frac{x}{2}\right)\ddot{\vartheta}_C+\frac{x}{2}\ddot{\vartheta}_1\right), \tag{20}$$

$$Fx-M_{0,1}=\mu_1 x^2\left(\left(\frac{L}{2}-\frac{x}{6}\right)\ddot{\vartheta}_C+\frac{x}{3}\ddot{\vartheta}_1\right). \tag{21}$$

Eliminating $\ddot{\vartheta}_1$ and $\ddot{\vartheta}_C$ from Eqs. (19) to (21) yields

$$F=\frac{3M_{0,1}}{x}-\frac{3(M_{0,1}-M_{0,2})}{2(L_1-x)^2}x^2 \tag{22}$$

This gives the relationship between the magnitude of the applied force and the hinge position in AC. With the value of F given, all the unknowns can be solved. It should be noted that when $\ddot{\vartheta}_1=0$, the double-hinge mechanism is at a transition state where it converts to the single-hinge mode at C, or vice versa. Denoting the dynamic load and position of H_1 at this transition state as F_{T1} and x_{T1}, from the Eqs. (19) to (21) we have

$$\frac{(3L_1-2x_{T1})x_{T1}^2}{2(L_1-x_{T1})^3}=\frac{M_{0,1}}{M_{0,1}-M_{0,2}}\equiv\bar{M},$$

or

$$2(\bar{M}-1)x_{T1}^3-3(\bar{M}-1)L_1x_{T1}^2+6\bar{M}L_1^2x_{T1}-2\bar{M}L_1^3=0 \tag{23}$$

and

$$F_{T1}=\frac{(2L_1-x_{T1})}{\left(L_1-\frac{2x_{T1}}{3}\right)x_{T1}}M_{0,1}. \tag{24}$$

Note that F_{T1} is a function of beam parameters and its expression is identical to Eq. (14), thus from the definition of F_3 in Eq. (15), we find that

$$F_3=F_{T1}. \tag{25}$$

This indicates that with $F_2\leq F<F_3$, a single hinge mode at C will happen, and with $F\geq F_3$, a double-hinge mode H_1-C will appear. The physical meaning of F_{T1} is that it is the least magnitude of F to have a double-hinge mode H_1-C and x_{T1} is the furthest location hinge H_1 may appear in AC from tip A. With increasing magnitude of $F(>F_{T1})$, hinge H_1 appears closer to A.

The validity of this double-hinge mode requires that the yield criterion at B is not violated, i.e.

$$Q_CL_2-M_{0,2}\leq M_{0,2},$$

or from Eqs. (18) and (19),

$$L_2\leq\frac{2M_{0,2}}{Q_C}=\frac{4(L_1-x)M_{0,2}}{3(M_{0,1}-M_{0,2})}. \tag{26}$$

As long as the above inequality is maintained, the double-hinge mechanism H_1-C is valid. Note that hinge position x is a function of F, hence the above inequality also becomes a function of F. The equation in (26) shows that the maximum Q_C happens at the transition state where $x=x_{T1}$, which has the maximum value of x, thus if

$$L_2<\bar{L}_2=\frac{4(L_1-x_{T1})M_{0,2}}{3(M_{0,1}-M_{0,2})}, \tag{27}$$

there will be not violation at B and the double-hinge mode H_1-C stands valid no matter how large the dynamic load is. $\bar{L}_2$ is the length limit of CB as discussed in the last section. Note that x_{T1} is determined by Eq. (23) and is only a function of beam parameters, so is $\bar{L}_2$. If Eq. (27) is not satisfied, there may be a yield at B and a triple-hinge mechanism H_1-C-B may appear.

A similar analysis was given by Hua, *et al.* (1988) for this particular mode. They also analyzed stepped beams with $M_{0,1}<M_{0,2}$, for which both single and double-hinge modes were reported and a complete set of solution was achieved.

2.2.2. $C-H_2$ mode

This mode happens when there are simultaneous failure at C and in L_2 if F is large enough and $L_2>\bar{L}_2$. Derivations of the governing equations are similar to the above. Assuming that the second hinge H_2 is formed at x in CB measured from C, $\dot{\vartheta}_C$ and $\dot{\vartheta}_2$ are the relative angular velocities at the hinges, as shown in Fig. 6, we have for CH_2

$$Q_C = \frac{\mu_2}{2} x^2 \ddot{\vartheta}_2, \tag{28}$$

$$Q_C x - M_{0,2} - M_{0,2} = \frac{\mu_2}{3} x^3 \ddot{\vartheta}_2; \tag{29}$$

for AC

$$F + Q_C = \mu_1 L_1 \left(-\left(x + \frac{L_1}{2} \right) \ddot{\vartheta}_2 + \frac{L_1}{2} \ddot{\vartheta}_C \right), \tag{30}$$

$$F L_1 - M_{0,2} = \mu_1 L_1^2 \left(-\left(\frac{x}{2} + \frac{L_1}{3} \right) \ddot{\vartheta}_2 + \frac{L_1}{3} \ddot{\vartheta}_C \right). \tag{31}$$

After simplification, it produces

$$F = 3M_{0,2} \left(\frac{1}{L_1} + \frac{4}{x} + \frac{2L_1}{x^2} \right). \tag{32}$$

This gives the relationship between the load magnitude and the hinge position in CB. Putting $x = L_2$, we have

$$F_5 = 3M_{0,2} \left(\frac{1}{L_1} + \frac{4}{L_2} + \frac{2L_1}{L_2^2} \right). \tag{33}$$

Therefore, under the load of $F_4 \leq F \leq F_5$, there will be a double-hinge mode C−B with a hinges at C and B simultaneously; and when $F > F_5$, the two hinges will be at C and x in CB, i.e., mode C−H_2. The position of hinge H_2 is determined by Eq. (32) when the value of F is given.

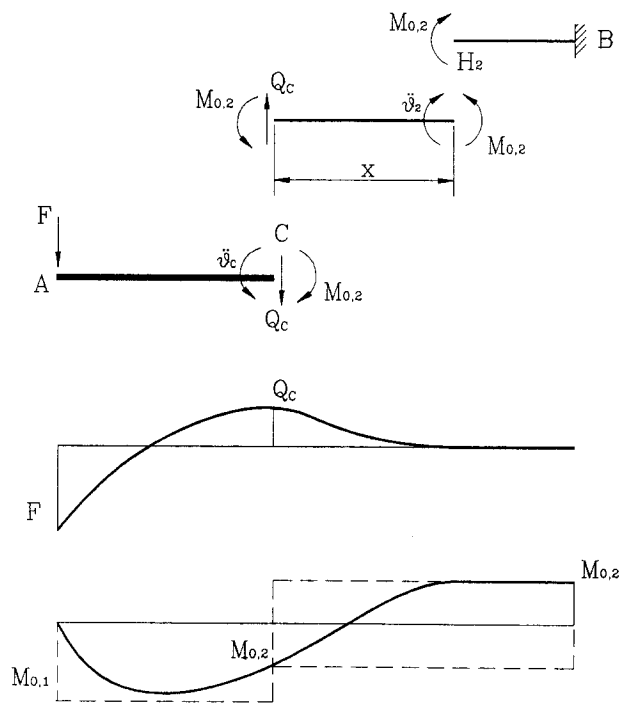

Fig. 6 Double-hinge mode C−H_2 and its shear force, bending moment diagrams.

As shown in Fig. 6, the maximum value of bending moment happens in AC, thus the validity of this mechanism depends on that the yield criterion in AC is not violated. To check this, let ζ be an arbitrary point in AC, then we have

$$F-Q_\zeta=\mu_1\zeta\left(-\left(x+L_1-\frac{\zeta}{2}\right)\ddot{\vartheta}_2+\left(L_1-\frac{\zeta}{2}\right)\ddot{\vartheta}_C\right), \tag{34}$$

$$F\zeta-M_\zeta=\frac{\mu_1}{2}\zeta^2\left(-\left(x+L_1-\frac{\zeta}{3}\right)\ddot{\vartheta}_2+\left(L_1-\frac{\zeta}{3}\right)\ddot{\vartheta}_C\right), \tag{35}$$

and

$$Q_\zeta+Q_C=\mu_1(L_1-\zeta)\left(-\left(x+\frac{L_1-\zeta}{2}\right)\ddot{\vartheta}_2+\left(\frac{L_1-\zeta}{2}\right)\ddot{\vartheta}_C\right). \tag{36}$$

If M_ζ reaches the maximum at ζ, $Q_\zeta=0$. Putting Eq. (28) into (36) yields

$$\ddot{\vartheta}_C=\frac{\frac{\mu_2}{\mu_1}x^2+2x(L_1-\zeta)-(L_1-\zeta)^2}{(L_1-\zeta)^2}\ddot{\vartheta}_2. \tag{37}$$

Eliminating F from Eqs. (34), (35) and with (37) gives

$$M_\zeta=\mu_1\zeta^2\left(-\frac{x}{2}+\frac{2x}{(L_1-\zeta)}\left(\frac{L_1}{2}-\frac{\zeta}{3}\right)+\frac{x^2}{(L_1-\zeta)^2}\left(\frac{L_1}{2}-\frac{\zeta}{3}\right)\right)\ddot{\vartheta}_2. \tag{38}$$

Finally, combining Eqs. (28), (29) and (38) leads to

$$M_\zeta=\zeta^2\left(-\frac{1}{2}+\frac{2}{(L_1-\zeta)}\left(\frac{L_1}{2}-\frac{\zeta}{3}\right)+\frac{x}{(L_1-\zeta)^2}\left(\frac{L_1}{2}-\frac{\zeta}{3}\right)\right)\frac{12\mu_1M_{0,2}}{\mu_2x^2}$$

Clearly, if

$$\zeta^2\left(-\frac{1}{2}+\frac{2}{(L_1-\zeta)}\left(\frac{L_1}{2}-\frac{\zeta}{3}\right)+\frac{x}{(L_1-\zeta)^2}\left(\frac{L_1}{2}-\frac{\zeta}{3}\right)\right)\frac{12\mu_1M_{0,2}}{\mu_2x^2}<M_{0,1}, \tag{39}$$

the double-hinge mechanism C$-$H$_2$ will remain valid when $F>F_5$.

The above inequality might not be maintained, then the yield criterion in AC will be violated. These will result in another hinge being introduced at the position where the maximum bending moment happens. Hence, a triple-hinge mechanism applies with three hinges appearing simultaneously in AC, at C and in CB. Details of this new triple-hinge mechanism are presented in section 2.3.

2.2.3. C$-$B mode

This double-hinge mode can be regarded as a special case of a C$-$H$_2$ mode. In the last section, the range of the dynamic load magnitude for this C$-$B mode has been identified as $F_4\leq F\leq F_5$ with $L_2>L_2$. There are two points which need to be addressed for this mode. First, when the second hinge is at B, there will be a concentrated shear force there, thus Eq. (28) should be changed as

$$Q_C-Q_B=\frac{\mu_2}{2}L_2^2\ddot{\vartheta}_B. \tag{40}$$

And in the rest of the governing equations, hinge position x should be replaced by L_2 and subscript 2 substituted by B. The unknowns are Q_C, $\ddot{\vartheta}_C$, Q_B and $\ddot{\vartheta}_B$ and they can be easily solved with the value of F given.

Secondly, the yield criterion in AC also needs to be checked. Eqs. (34) to (36) are modified as

$$F-Q_\zeta=\mu_1\zeta\left(-\left(L_2+L_1-\frac{\zeta}{2}\right)\ddot{\vartheta}_B+\left(L_1-\frac{\zeta}{2}\right)\ddot{\vartheta}_C\right), \tag{41}$$

$$F\zeta-M_\zeta=\frac{\mu_1}{2}\zeta^2\left(-\left(L_2+L_1-\frac{\zeta}{3}\right)\ddot{\vartheta}_B+\left(L_1-\frac{\zeta}{3}\right)\ddot{\vartheta}_C\right), \tag{42}$$

and

$$Q_\zeta+Q_C=\mu_1(L_1-\zeta)\left(-\left(L_2+\frac{L_1-\zeta}{2}\right)\ddot{\vartheta}_B+\left(\frac{L_1-\zeta}{2}\right)\ddot{\vartheta}_C\right), \tag{43}$$

where ζ is an arbitrary point in AC measured from A. If M_ζ reaches its maximum at ζ, $Q_\zeta=0$. After simplification, we have

$$\ddot{\vartheta}_C=\frac{\frac{4M_{0.2}}{\mu_1L_2}\left(\frac{\mu_2L_2^2}{3\mu_1L_1^2}+\frac{L_2}{L_1}+\frac{1}{6}\right)-\frac{6M_{0.2}}{\mu_1L_1^2}\left(\frac{2}{L_2}+\frac{1}{L_1}\right)\left[(L_1-\zeta)^2+2(L_1-\zeta)L_2+\frac{2\mu_2}{3\mu_1}L_2^2\right]}{2(L_1-\zeta)L_2+\frac{2\mu_2}{3\mu_1}L_2^2}$$

$$\ddot{\vartheta}_B=\frac{(L_1-\zeta)^2\ddot{\vartheta}_C-\frac{4M_{0.2}}{\mu_1L_2}}{(L_1-\zeta)^2+2(L_1-\zeta)L_2+\frac{2\mu_2}{3\mu_1}L_2^2}$$

$$M_\zeta=\mu_1\zeta^2\left[-\left(\frac{L_2}{2}+\frac{L_1}{2}-\frac{\zeta}{3}\right)\ddot{\vartheta}_B+\left(\frac{L_1}{2}-\frac{\zeta}{3}\right)\ddot{\vartheta}_C\right]. \tag{44}$$

Substituting $\ddot{\vartheta}_C$ and $\ddot{\vartheta}_B$ into Eq. (44) gives $M_\zeta=M(\zeta)$. If $M_\zeta<M_{0.1}$, the double-hinge mode C−B is valid; otherwise, the yield criterion in AC is violated and a new hinge should be introduced there, leading to the mode H_1−C−B.

There is no need to use Eqs. (39) and (44) to examine the validity of modes C−H_2 and C−B. Boundaries of load magnitude will be derived from corresponding triple-hinge mechanisms, as will be seen in the following section, which define the load ranges of valid double-hinge modes.

2.3. Triple-hinge mechanisms

As discussed in above sections, there exist two possible triple-hinge modes, H_1−C−H_2 and H_1−C−B. It will be shown in the following that which mode appears depends on the length of CB and with these two modes, a complete family of yield mechanism will be achieved and no further modes are needed.

2.3.1. H_1−C−H_2 mode

The overall analytical approach is similar to other sections of this paper. Assuming that the

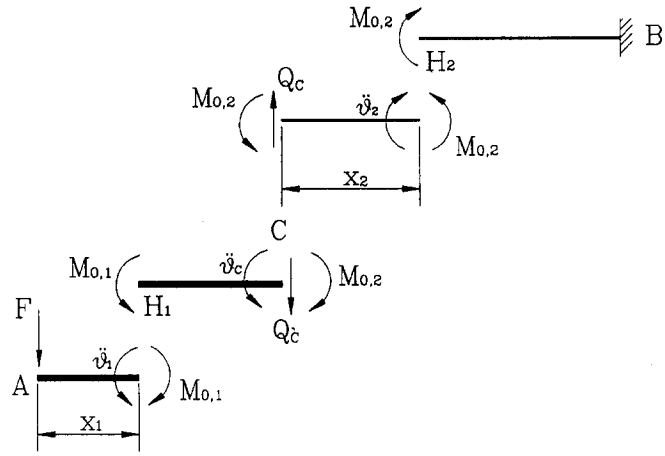

Fig. 7 Triple-hinge mode H_1-C-H_2.

hinge in AC, H_1 and in CB, H_2 is formed at x_1 and x_2, measured from A and C, respectively, and there is a third hinge at C shown in Fig. 7, $\ddot{\vartheta}_1$, $\ddot{\vartheta}_C$ and $\ddot{\vartheta}_2$ are the relative angular velocities across the corresponding hinges.

Equations of motion for each segment lead to the following: for segment CH_2

$$Q_C=\frac{\mu_2}{2}x_2^2\ddot{\vartheta}_2, \tag{45}$$

$$Q_Cx_2-M_{0,2}-M_{0,2}=\frac{\mu_2}{3}x_2^3\ddot{\vartheta}_2; \tag{46}$$

for segment H_1C

$$Q_C=\mu_1(L_1-x_1)\left(-\left(x_2+\frac{L_1-x_1}{2}\right)\ddot{\vartheta}_2+\left(\frac{L_1-x_1}{2}\right)\ddot{\vartheta}_C\right), \tag{47}$$

$$M_{0,1}-M_{0,2}=\mu_1(L_1-x_1)^2\left(-\left(\frac{x_2}{2}+\frac{L_1-x_1}{3}\right)\ddot{\vartheta}_2+\left(\frac{L_1-x_1}{3}\right)\ddot{\vartheta}_C\right); \tag{48}$$

for segment AH_1

$$F=\mu_1x_1\left(-\left(x_2+L_1-\frac{x_1}{2}\right)\ddot{\vartheta}_2+\left(L_1+\frac{x_1}{2}\right)\ddot{\vartheta}_C+\frac{x_1}{2}\ddot{\vartheta}_1\right), \tag{49}$$

$$Fx_1-M_{0,1}=\frac{\mu_1}{2}x_1^2\left(-\left(x_2+L_1-\frac{x_1}{3}\right)\ddot{\vartheta}_2+\left(L_1+\frac{x_1}{3}\right)\ddot{\vartheta}_C+\frac{2x_1}{3}\ddot{\vartheta}_1\right). \tag{50}$$

From Eqs. (45) and (46),

$$\ddot{\vartheta}_2=\frac{12M_{0,2}}{\mu_2x_2^3}, \tag{51}$$

Combining Eqs. (45) and (47) gives

$$\ddot{\vartheta}_C=\frac{\frac{\mu_2}{\mu_1}x_2^2+2x_2(L_1-x_1)-(L_1-x_1)^2}{(L_1-x_1)^2}\ddot{\vartheta}_2. \tag{52}$$

And submitting Eqs. (51) and (52) into (48) produces

$$(L_1-x_1)^2+\frac{2\mu_1}{\mu_2}(L_1-x_1)x_2-\frac{\mu_1(M_{0,1}-M_{0,2})}{2\mu_2 M_{0,2}}x_2^2=0. \tag{53}$$

This shows a linear relationship between the positions of the two hinges in AC and CB,

$$x_1=L_1-Kx_2, \tag{54}$$

where

$$K=\frac{\mu_1}{\mu_2}\left(\sqrt{1+\frac{\mu_2(M_{0,1}-M_{0,2})}{\mu_1 M_{0,2}}}-1\right).$$

Eliminating $\ddot{\vartheta}_1$ from Eqs. (49) and (50) gives

$$F=\frac{3M_{0,1}}{x_1}-\frac{6M_{0,2}[\mu_1(L_1-x_1)+\mu_2 x_2]x_1}{\mu_2(L_1-x_1)x_2^2}.$$

With the linear relationship Eq. (54), it produces

$$F=\frac{3M_{0,1}}{x_1}-\frac{6M_{0,2}K(\mu_1 K+\mu_2)x_1}{\mu_2(L_1-x_1)^2}, \tag{55}$$

or

$$F=\frac{3M_{0,1}}{(L_1-Kx_2)}-\frac{6M_{0,2}(\mu_1 K+\mu_2)(L_1-Kx_2)}{\mu_2 Kx_2^2}. \tag{56}$$

The above equations give the required relationships between the hinge positions and load magnitude. It shows that when the load is larger, x_1 is smaller and x_2 is larger, indicating H_1 and H_2 appearing farther away from C in terms of the increasing magnitude of the load. The limit positions of H_1 and H_2 are 0 and L_1/K respectively, happening at $F\to\infty$. However if $L_2\leq L_1/K$, the hinge in CB may appear at B, then we have

$$F_7=\frac{3M_{0,1}}{(L_1-KL_2)}-\frac{6M_{0,2}(\mu_1 K+\mu_2)(L_1-KL_2)}{\mu_2 KL_2^2}. \tag{57}$$

There is also a transition state where $\ddot{\vartheta}_1$ is equal zero, then the triple-hinge mode H_1-C-H_2 becomes a double-hinge mode $C-H_2$, or vice versa. Denoting the value of F, x_1 and x_2 at this state as F_6, λ_{T1} and λ_{T2}, respectively, and putting $\ddot{\vartheta}_1=0$ in the governing equations, we have

$$M_{0,1}=\lambda_{T1}^2\left(-\frac{1}{2}+\frac{2}{(L_1-\lambda_{T1})}\left(\frac{L_1}{2}-\frac{\lambda_{T1}}{3}\right)+\frac{\lambda_{T2}}{(L_1-\lambda_{T1})^2}\left(\frac{L_1}{2}-\frac{\lambda_{T1}}{3}\right)\right)\frac{12\mu_1 M_{0,2}}{\mu_2\lambda_{T2}^2}. \tag{58}$$

It is noted that the right-hand side of Eq. (57) is identical to the left-hand side of Eq. (39), comfirming that when $M_\zeta=M_{0,1}$, the double-hinge mode $C-H_2$ is not valid any more and a triple-hinge mode H_1-C-H_2 appears. Substituting Eq. (54) into (58), the transition hinge positions can be obtained,

$$\left(2(2+K)K\frac{\mu_1 M_{0,2}}{\mu_2 M_{0,1}}-1\right)\lambda_{T1}^3-3\left(2(K+1)K\frac{\mu_1 M_{0,2}}{\mu_2 M_{0,1}}-1\right)L_1\lambda_{T1}^2-3L_1^2\lambda_{T1}+L_1^3=0. \tag{59}$$

The corresponding value of F at this state can also be derived from Eq. (50)

$$F_6=\frac{3M_{0,1}}{\lambda_{T1}}-\frac{6M_{0,2}K(\mu_1K+\mu_2)\lambda_{T1}}{\mu_2(L_1-\lambda_{T1})^2} \tag{60}$$

The physical meaning of F_6 is that it is the least magnitude of the dynamic force required for this triple-hinge mechanism, and for λ_{T1} (and λ_{T2} as well), it is the closest position to C a hinge may possibly appear in AC (or CB). It is now clear that for a double-hinge mode C−H_2, the load range is $F_5<F<F_6$, and for a triple-hinge mode H_1−C−H_2, $F\geq F_6$.

The requirement on the length of CB in this triple-hinge mode is given by

$$L_2>\lambda_{T2}=\frac{L_1-\lambda_{T1}}{K}. \tag{61}$$

As long as L_2 satisfies Eq. (61), mode H_1−C−H_2 will appear when $F\geq F_6$; otherwise, there will be a different triple-hinge mode H_1−C−B with the third hinge appearing at B.

2.3.2. H_1−C−B mode

This triple-hinge mechanism may actually appear in two situations: first as stated in the last section, when Eq. (44) is not satisfied a double-hinge mode C−B turns into a triple-hinge mode; the second situation happens when $\lambda_{T2}<L_2\leq L_1/K$ and $F\geq F_7$ as given in Eq. (61), the hinge in CB for a triple-hinge mode will appear at B. All the governing equations for this mode are virtually the same as for mode H_1−C−H_2 with substitutions of x_2 by L_2 and subscript 2 by B. The only exception is Eq. (50) in which a shear force at the beam root should be introduced,

$$Q_C-Q_B=\frac{\mu_2}{2}x_B^2\ddot{\vartheta}_B. \tag{62}$$

After a lengthy manipulation, we obtain

$$\ddot{\vartheta}_C=\frac{\frac{M_{0,1}-M_{0,2}}{(L_1-x_1)^2}\left[(L_1-x_1)^2+2(L_1-x_1)L_2+\frac{2\mu_2}{3\mu_1}L_2^2\right]-\frac{4M_{0,2}}{L_2}\left(\frac{L_2}{2}+\frac{L_1-x_1}{3}\right)}{\frac{\mu_2L_2}{3}(L_1-x_1)\left(\frac{2\mu_2}{\mu_1}L_2+\frac{L_1-x_1}{2}\right)}, \tag{63}$$

$$\ddot{\vartheta}_B=\frac{(L_1-x_1)^2\ddot{\vartheta}_C-\frac{4M_{0,2}}{\mu_1L_2}}{(L_1-x_1)^2+2(L_1-x_1)L_2+\frac{2\mu_2}{3\mu_1}L_2^2}, \tag{64}$$

$$F=\frac{3M_{0,1}}{x_1}-\frac{\mu_1x_1}{2}\left[-(L_2+L_1-x_1)\ddot{\vartheta}_B+(L_1-x_1)\ddot{\vartheta}_C\right]. \tag{65}$$

Putting Eqs. (63) and (64) into (65) gives the required relationship between F and x_1. With the value of F given, all unknowns can be solved.

There is also a transition state in this mechanism at which the triple-hinge mode H_1−C−B changes to a double-hinge mode C−B, or vice versa. Note that this transition state only applies to the first situation as stated at the beginning of this section where mode C−B appears first. Denoting F_8 and η_{T1} as the load magnitude and the hinge position in AC at this transition state and letting $\ddot{\vartheta}_1=0$, it is not difficult to get

$$M_{0,1}=\mu_1\eta_{T1}^2\left[-\left(\frac{L_2}{2}+\frac{L_1}{2}-\frac{\eta_{T1}}{3}\right)\ddot{\vartheta}_B+\left(\frac{L_1}{2}-\frac{\eta_{T1}}{3}\right)\ddot{\vartheta}_C\right], \tag{66}$$

where the angular accelerations are given by Eqs. (63) and (64) with x_1 being replaced by η_{T1}. Note that the left-hand side of Eq. (66) is identical to that of Eq. (44), confirming the transition between the modes C−B and H_1−C−B. When η_{T1} is obtained from Eq. (66) accordingly, from Eq. (65) we have

$$F_8 = F(\eta_{T1}). \tag{67}$$

F_8 is the least value of force needed to have this triple-hinge mode. Therefore, with $F_4 \leq F < F_8$, a double-hinge mode C−B will appear; and when $F \geq F_8$, a triple-hinge mode H_1−C−B will show.

3. Discussions

In order to summarize the extensive results derived above, three categories of stepped beams are identified according to the geometry of the beam which determines the possible yield mechanisms. For each category, all possible yield modes are listed in order of load magnitude.

The results obtained in this paper show that various modes may appear in certain cases as the response of a stepped straight cantilever subjected to a step tip force. A family of solutions including single, double- and triple-hinge mechanisms, has been constructed for all geometry. All the mechanisms are both statically and kinetically admissible. It has been shown that the maximum number of plastic hinges which may appear simultaneously in the beam is three and no further hinges are needed, regardless of the magnitude of the dynamic load. The geometrical restrictions divide the response modes into three categories from which it is clear that the

(1) Category 1. For those satisfying $L_2 \leq \bar{L}_2$, seeing Eq. (27) for definition of $\bar{L}_2$

Mode	Mode of response	Range of F	Related equations
I	No hinge	$F < F_0$	Eq. (2)
II	Single hinge B	$F_0 \leq F \leq F_1$	Eq. (6)
III	Single hinge H_2	$F_1 < F < F_2$	Eq. (7)
IV	Single hinge C	$F_2 \leq F < F_3$	Eq. (25)
V	Double-hinge H_1−C	$F \geq F_3$	

Fig. 8 illustrates the results of Category 1.

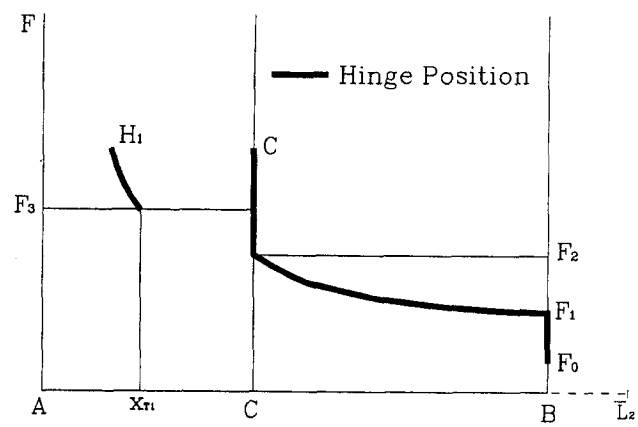

Fig. 8 Mode pattern of category 1. Hinge positions for increasing magnitude of F.

(2) Category 2. For those with $\bar{L}_2 < L_2 \leq \lambda_{T2}$, λ_{T2} being given in Eq. (61)

Mode	Mode of response	Range of F	Related equations
I	No hinge	$F<F_0$	Eq. (2)
II	Single hinge B	$F_0 \leq F \leq F_1$	Eq. (6)
III	Single hinge H_2	$F_1 < F < F_2$	Eq. (7)
IV	Single hinge C	$F_2 \leq F < F_4$	Eq. (17)
V	Double-hinge C−B	$F_4 \leq F < F_8$	Eq. (67)
VI	Triple-hinge H_1−C−B	$F \geq F_8$	

A similar illustration can also be constructed as shown in Fig. 9.

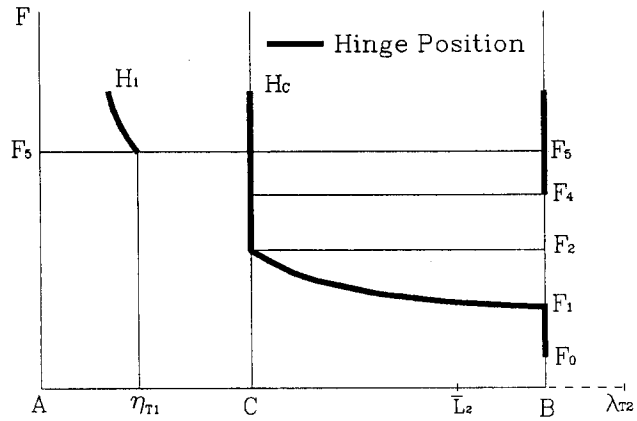

Fig. 9 Mode pattern of category 2. Hinge positions for increasing magnitude of F.

(3) Category 3. For stepped beams with $\lambda_{T2} < L_2 \leq L_1/K$, we have

Mode	Mode of response	Range of F	Related equations
I	No hinge	$F<F_0$	Eq. (2)
II	Single hinge B	$F_0 \leq F \leq F_1$	Eq. (6)
III	Single hinge H_2	$F_1 < F < F_2$	Eq. (7)
IV	Single hinge C	$F_2 \leq F < F_4$	Eq. (17)
V	Double-hinge C−B	$F_4 \leq F \leq F_5$	Eq. (33)
VI	Double-hinge C−H_2	$F_5 < F < F_6$	Eq. (60)
VII	Triple-hinge H_1−C−H_2	$F_6 \leq F < F_7$	Eq. (57)
VIII	Triple-hinge H_1−C−B	$F \geq F_7$	

For those with $L_2 > L_1/K$, Mode VII becomes Triple-hinge H_1−C−H_2; $F \geq F_6$ and Mode VIII does not exist. Fig. 10 shows an illustration of this category.

triple-hinge mechanism will not necessarily appear in every case.

None of the single hinge mode may become an ultimate yield mechanism, which is defined as the mode when the dynamic load magnitude is indefinitely high. With beam dimensions permitting, double-hinge mode H_1−C and the two triple-hinge modes can all be an ultimate mode. The remaining two double-hinge modes are only intermediate modes in Category 2 and 3. Note that the values of load range boundaries for each mode are only determined by beam parameters. Using a shear force diagram, Fig. 11 reveals the interchanging relationships amongst the various yield mechanisms.

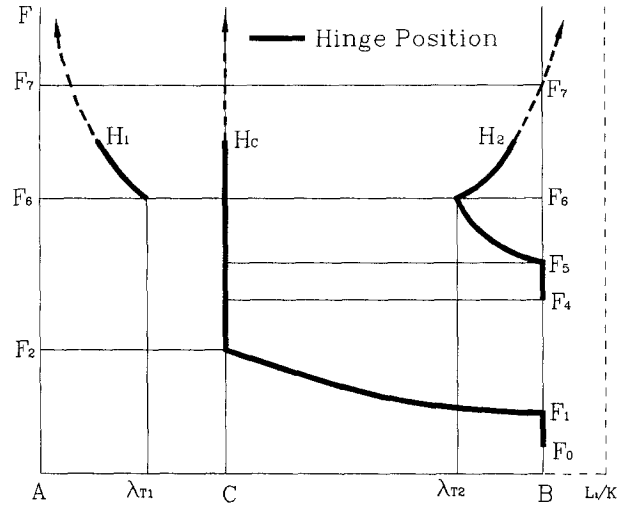

Fig. 10 Mode pattern of category 3. Hinge positions for increasing magnitude of F.

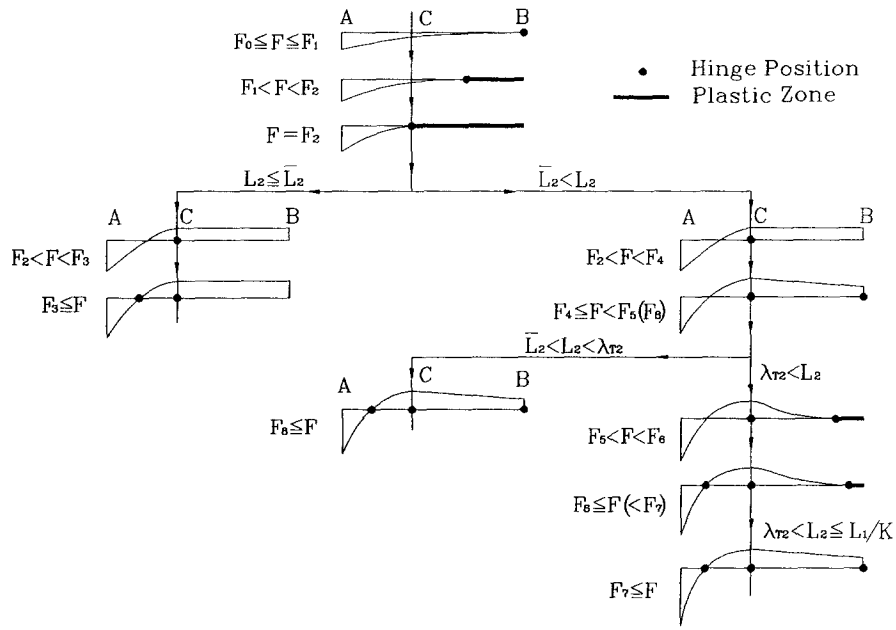

Fig. 11 Shear force diagram. Interchanging relationships amongst different modes.

If the tip force is applied and maintained for only a finite duration, i.e. a rectangular pulse, assuming that a triple-hinge mode H_1-C-H_2 is initiated during the pulse, after the force is removed, the shear force distribution will be disturbed and hinges H_1 and H_2 will have to travel along the beam segments. This moving phenomenon of the plastic hinge may also be caused by changing magnitude of the load and by alllowing large deflections of the beam to occur. Details of this transient response of stepped beams are under studies.

Notations

F	dynamic load at the beam tip.
L	length of beam segment;
M	bending moment;
$M_{0,1}$, $M_{0,2}$	dynamic fully plastic bending moments of segment AC and CB, respectively;
Q	shear force;
x	hinge positions;
η, λ	transitions positions of hinges in triple-hinge modes;
μ	density per unit length of beam segment;
ϑ	angular velocity due to bending across a hinge.

Subscripts

1	variables of segment AC;
2	variables of segment CB;
B	variables at B;
C	variables at C;
T	variables at transition state of a yield mode.

Acknowledgements

The author is grateful to the reviewers for their helpful comments on the original manuscript.

References

Hua, Y. L., Yu, T. X. and Reid, S. R. (1988), "Double-hinge modes in the dynamic response of plastic cantilever beams subjected to step loading", *Int. J. Impact Engng.*, **7**, 401-414.

Johnson, W. (1972), *Impact strength of materials*, Arnold, E., London.

Lee, E. H. and Symonds, P. S. (1952), "Large plastic deformation of beams under transverse impact", *J. Appl. Mech.*, **19**, 308-314.

Martin, J. B. (1964), "The plastic deformation of a bent cantilever", Division of Engineering, Brown Univ. Report N87, GP 1115/15.

Reid, S. R., Wang, B. and Yu, T. X. (1995a), "Yield mechanisms of a bent cantilever beam subjected to a constant out-of-plane tip force", *Int. J. Impact Engng.*, **16**, 49-73.

Reid, S. R., Wang, B. and Hua, Y. L. (1995b), "Triple plastic hinge mechanism for a bent cantilever beam subjected to an out-of-plane tip force pulse of finite duration", *Int. J. Impact Engng.*, **16**, 75-93.

Yu, T. X., Hua, Y. L. and Johnson, W. (1985), "The plastic hinge position in a circular cantilever when struck normal to its plane by a constant jet at its tip", *Int. J. Impact Engng.*, **3**, 143-154.

Wang, B., Yu, T. X. and Reid, S. R. (1993), "Out-of-plane impulsive loading of a right-angled bent cantilever beam", *Advances in Engineering Plasticity and its Application*, Lee, W. B. (Ed.), Elsevier, 491-496.

Wang, B., (1994), "Response of a bent cantilever to an impulsive load applied at its tip normal to its plane", *Int. J. Solids Structures*, **31**, 1377-1392.